

# SnowFormer: Scale-aware Transformer via Context Interaction for Single Image Desnowing

Sixiang Chen<sup>\*1</sup>, Tian Ye<sup>\*1</sup>, Yun Liu<sup>\*2</sup>, Erkang Chen<sup>†1</sup>, Jun Shi<sup>3</sup>, Jingchun Zhou<sup>4</sup>

<sup>1</sup>School of Ocean Information Engineering, Jimei University, Xiamen, China

<sup>2</sup>Southwest University School of Artificial Intelligence, Chongqing, China

<sup>3</sup>Xinjiang University School, Xinjiang, China

<sup>4</sup>Dalian Maritime University School, Dalian, China

## Abstract

Single image desnowing is a common yet challenging task. The complex snow degradations and diverse degradation scales demand strong representation ability. In order for the desnowing network to see various snow degradations and model the context interaction of local details and global information, we propose a powerful architecture dubbed as SnowFormer. First, it performs Scale-aware Feature Aggregation in the encoder to capture rich snow information of various degradations. Second, in order to tackle with large-scale degradation, it uses a novel Context Interaction Transformer Block in the decoder, which conducts context interaction of local details and global information from previous scale-aware feature aggregation in global context interaction. And the introduction of local context interaction improves recovery of scene details. Third, we devise a Heterogeneous Feature Projection Head which progressively fuse features from both the encoder and decoder and project the refined feature into the clean image. Extensive experiments demonstrate that the proposed SnowFormer achieves significant improvements over other SOTA methods. Compared with SOTA single image desnowing method HDCW-Net, it boosts the PSNR metric by 9.2dB on the CSD testset. Moreover, it also achieves a 5.13dB increase in PSNR compared with general image restoration architecture NAFNet, which verifies the strong representation ability of our SnowFormer for snow removal task. The code is released in <https://github.com/Ephemeral182/SnowFormer>.

## Introduction

Degraded images are detrimental for high-level vision tasks, such as object detection (Carion et al. 2020) and image segmentation (Chen et al. 2021a). Single image desnowing aims to reconstruct the clean image from a snow degraded version, which is challenging due to the complex snow degradation and diverse degradation scales. According to the previous desnowing works (Chen et al. 2020), snow image formation can be expressed as:

$$I(x) = K(x)T(x) + A(x)(1 - T(x)), \quad (1)$$

where the  $I(x)$  denotes the snow image,  $T(x)$  and  $A(x)$  represent the transmission map and atmospheric light respec-

<sup>\*</sup>These authors contributed equally.

<sup>†</sup>Corresponding Author.

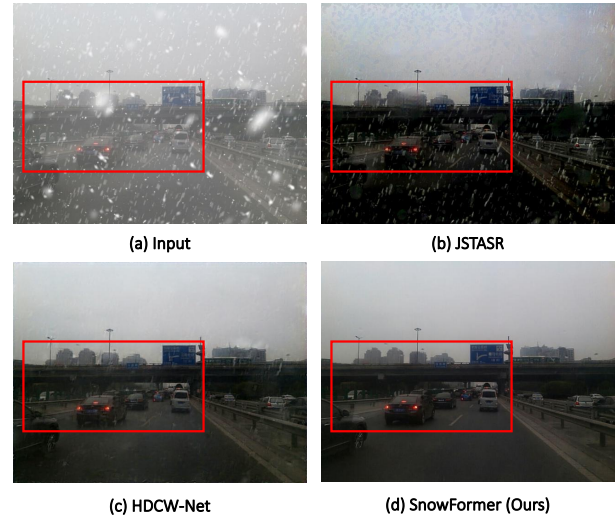


Figure 1: Visual comparison of state-of-the-art single image desnowing methods and our SnowFormer. (a) is the input snow image. (b) and (c) are results of JSTASR (Chen et al. 2020) and HDCW-Net (Chen et al. 2021c) algorithms. (d) is the result of our SnowFormer.

tively.  $K(x)$ , the veiling-free snow scene, can be decomposed as:  $K(x) = J(x)(1 - Z(x)R(x)) + C(x)Z(x)R(x)$ , where  $R(x)$  is the binary mask image which presents the location information of snow,  $Z(x)$  and  $C(x)$  denote the chromatic aberration image and the snow mask.

From the above formation model, the degradation of snow scene is complex. Visually speaking, it can be seen from Fig.1(a) that snow degradation includes snow streaks of different sizes, a few snow spots, and hazy fog morbidly overlaid on the scene. The composite degraded snow scene requires that the desnowing network needs to pay attention to different degradation information. JSTASR (Chen et al. 2020) proposed a method for dealing with the veiling effect and image inpainting from the degradation version. HDCW-Net (Chen et al. 2021c) adopted the dual-tree complex wavelet transform to decompose the snow image and designed a high-frequency reconstruction network and a low-frequency reconstruction network to process snow par-

ticles and large-scale degradation. However, as shown in Fig.1(b) and (c), it is difficult for previous methods to handle various degradation information simultaneously. Therefore, we present our motivation:

- *How to design an effective and efficient snow removal network that can see various kinds of degradations in snow scenes?*

We believe that the context interaction of local details and global information is essential for single image desnowing. Compared with utilizing operations such as wavelet transform (Chen et al. 2021c), Fourier transform (Ye et al. 2022), ViT (Dosovitskiy et al. 2020) design can capture long-distance dependencies well. PVT (Wang et al. 2021) proposed a pyramidal architecture to gradually expand the receptive field and perform global modeling. Swin Transformer (Liu et al. 2021) divided the image into different windows and limited the self-attention operation inside the window to reduce computational overhead, which achieved advanced performance. Nevertheless, differ from high-level vision tasks, recovering clean images from adverse snow scenes using ViT still faces the following issues: (i) **Plain Vit lacks the ability of modeling context interaction of local details and global information.** (ii) **The large computational overhead of ViT is unfriendly for low-level vision tasks.**

To solve the above issues, in this paper, we propose SnowFormer, a careful design consistent with our motivation. At the same time, the parameters and the amount of computation are competitive compared to other SOTA methods. Specifically, we devise a Scale-aware Aggregation Module (SaA) in the encoder part, aggregating different degradation information and enriching the representation ability of the scale-aware feature. Next, in the decoder part, we propose a Context Interaction Transformer Block (CITB). It consists of window-based local context interactions and global context interactions whose query is generated by the scale-aware feature. It is worth mentioning that the scale-aware-guided cross self-attention mechanism can improve the exchange between local details and global information. In addition, we offer the Heterogeneous Feature Projection Head (HFPH), which aims to deal with the residual degradation problem in the recovering processing. We use the heterogeneous features of each stage for progressive fusion and refinement. Compared with the direct single output decoder feature as input (Zamir et al. 2021), our design can better obtain snow features at different stages, promoting the refinement block and projecting it to a clean image.

Overall, our contributions can be summarized as follows:

- To enhance the feature representation of various snow degradations and avoid the loss of small degradations due to repeated down-sampling operations, we propose a Scale-aware Aggregation Module.
- We propose the Context Interaction Transformer Block, which not only improves local modeling, but also enables context interaction of local details and global information by using scale-aware-based cross self-attention.
- A Heterogeneous Feature Projection Head is proposed to handle the residual degradation, where heterogeneous

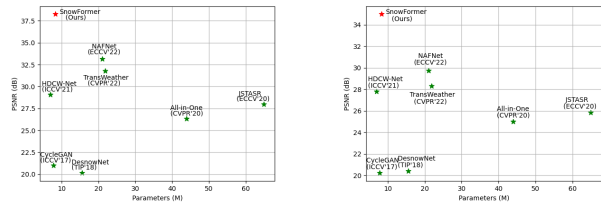


Figure 2: Trade-off between PSNR performance and the number of parameters on CSD (Chen et al. 2021c) dataset (left) and SRRS (Chen et al. 2020) dataset (right). The results show the superiority of our model compared with other SOTA desnowing methods.

features at different stages are progressively refined and projected to the clean image.

## Related Works

### Single Image Desnowing

(i) **Physics-based Methods:** In early days, most desnowing approaches were based on some physical models and leveraged prior knowledge. (Pei, Tsai, and Lee 2014) used image priors of saturation and visibility in snow scenes to remove snow particles. (Zheng et al. 2013) considered the influence of background edges and differences in rain streaks and applied a multi-guided filter to extract snow features, which can separate snow components from the background. (Wang et al. 2017) proposed a hierarchical scheme that enables dictionary learning and snow component decomposition. (ii) **Data-driven Methods:** With the rapid development of deep learning, learning-based approaches have achieved remarkable results. As the first snow removal network dubbed as DesnowNet (Liu et al. 2018) designed a multi-stage model to remove snow particles and snowflakes progressively. All-in-one bad weather removal network (Li, Tan, and Cheong 2020) offered multiple specific encoders to simultaneously handle various degradations, which can recover different ill-posed weather issues. JSTASR (Chen et al. 2020) considered the veiling effect and the diversity of snow cover and proposed a multi-scale snow network for snow removal from a single image. HDCW-Net (Chen et al. 2021c) embedded the dual-tree wavelet transform into the network architecture. In addition, the authors also designed a prior-based loss called contradictory channel to perform image snow removal. TransWeather (Valanarasu, Yasarla, and Patel 2022) utilized the ViT as the backbone and proposed a weather type decoder to promote processing multiple adverse weather scenes, which achieves non-trivial improvements.

### Vision Transformer

Recently, inspired by the remarkable successes of transformers in natural language processing, vision transformer (Dosovitskiy et al. 2020) (ViT) gradually has been applied for computer vision tasks. Compared with the dominant convolutional neural networks (CNNs), ViT can offer

the powerful ability of global feature modeling. Using this advantage, several ViT-based networks have achieved impressive effects in various fields (Liu et al. 2021; Lee et al. 2021; Wang et al. 2021; Chen, Fan, and Panda 2021; Mehta and Rastegari 2021). PVT (Wang et al. 2021) presented a pyramid architecture to progressively enlarge the receptive field and reduce the size of feature map, improving the performance and mitigating the computational overhead. Swin-Transformer (Liu et al. 2021) partitioned an image into windows and restricted self-attention operation inside each window, which significantly reduces the computational complexity. To obtain global modeling capability, it adopt a window shifting operation, enabling interaction among nearby windows. CrossVit (Chen, Fan, and Panda 2021) made use of the projection from different features to perform a cross self-attention mechanism, which can utilize the global information representation to a greater extent.

Besides high-level tasks, recently ViT has been applied for low-level image restoration due to its advantage of global long-distance dependencies (Zamir et al. 2021; Wang et al. 2022; Song et al. 2022; Valanarasu, Yasarla, and Patel 2022; Lee et al. 2022). Uformer (Wang et al. 2022) utilized the Swin-transformer module to adopt it in a U-shape (Ronneberger, Fischer, and Brox 2015) architecture for image restoration. Restormer (Zamir et al. 2021) proposed channel dimension self-attention operation to capture the channel information. However, these overall ViT-based architectures may lead to huge computational complexity. For the task of single image dehazing, Dehazeformer (Song et al. 2022) designed a Swin-based model which utilizes the padding operation to improve the edge repair effect. In this work, we believe that global and local information are both vital for image desnowing. We propose a scale-aware Transformer with context interaction, which greatly enhances the global attention capability for snow removal. Furthermore, a novel heterogeneous feature refinement is presented to optimize the embedded features of CNNs and ViT.

## Method

### SnowFormer

As shown in Fig.3, the overall structure of our proposed SnowFormer is a heterogeneous U-shaped architecture that consists of a CNNs-based encoder and a ViT-based decoder. Specifically, we utilize the Scale-aware Aggregation Module to capture the local information and integrate multi-scale features, which can aggregate various snow degradation features while avoiding the problem of feature loss due to repeated down-sampling. Next, we feed it to the latent layer for global context modeling. For the decoder design, we believe that for the complex degradation process in snow removal, it is essential to utilize scale-aware features for local and global context interactions. Therefore, we employ Context Interaction Transformer Block to reconstruct the image features. In addition, we devise a Heterogeneous Feature Projection Head (HFPH) that fuses and refines the heterogeneous features. Finally, it projects the optimized feature into the clean image.

### Scale-aware Aggregation Module

For the encoder, we adopt a spindle-shaped DWConv $3\times 3$ -LN-GULE-DWConv $3\times 3$  block for local feature extraction and gradually down-sampled the features while expanding the local receptive field. However, there are still two problems needed to be considered. (i) Various degradations in the snow scene are overlaid on the clean image, which is challenging for restoration. (ii) Information loss is unavoidable as the resolution is gradually reduced, which makes this plain encoder structure difficult to capture small degradations, such as snow spots and snow streaks. To tackle these problems, we propose the Scale-aware Aggregation which extracts various and multi-scale degradation information by aggregating hierarchical features to form the scale-aware feature. Specifically, the max-pooling and Conv $1\times 1$  operations are utilized to align the feature size of each stage. The proposed Scale-aware Aggregation operation can be expressed as:

$$X_{Fi} \in \mathbb{R}^{\frac{H}{16} \times \frac{H}{16} \times 16C} = X_i \in \mathbb{R}^{\frac{H}{2^i} \times \frac{W}{2^i} \times 2^i C} \downarrow, \quad (2)$$

$$X_F = \sum_{i=0}^3 X_{Fi} + X_4, \quad (3)$$

where  $\downarrow$  represents the combined operations of max-pooling and Conv $1\times 1$ ,  $i$  denotes the  $i$ -th layer of the encoder.  $H$ ,  $W$  and  $C$  mean the height, width and channel dimension of feature in the first layer.  $X_F$  represents the final feature after scale-aware aggregation operation.

We subsequently apply a multi-head self-attention block (Dosovitskiy et al. 2020) on  $X_F$  for global modeling, outputting scale-aware information for the cross self-attention of context interaction. Detailed explanation and implementation of this block are provided in the supplementary material.

### Context Interaction Transformer Block

**Local Context Interaction Module** For single image desnowing, local information is the foundation for removing the ill-pose degradations (Chen et al. 2021c). Local context interaction improves the effects of detail restoration from complex snow images. Compared with CNNs, local self-attention shows more strong interaction ability. Inspired by (Liu et al. 2021), we employed the window-based self-attention to model the local context interaction in the decoder part, which achieves the trade-off between the performance and computational complexity. We describe our Local Context Interaction module as follows:

$$\hat{X}_w = X_w + \text{W-MSA} (X_w), \quad (4)$$

$$X_l = \hat{X}_w + \text{MLP} (\hat{X}_w), \quad (5)$$

where  $\hat{X}_w$  and  $X_l$  denote the output feature of W-MSA and MLP modules. W-MSA and MLP represent the window-based multi-head self-attention and the multilayer perceptron feed-forward network.

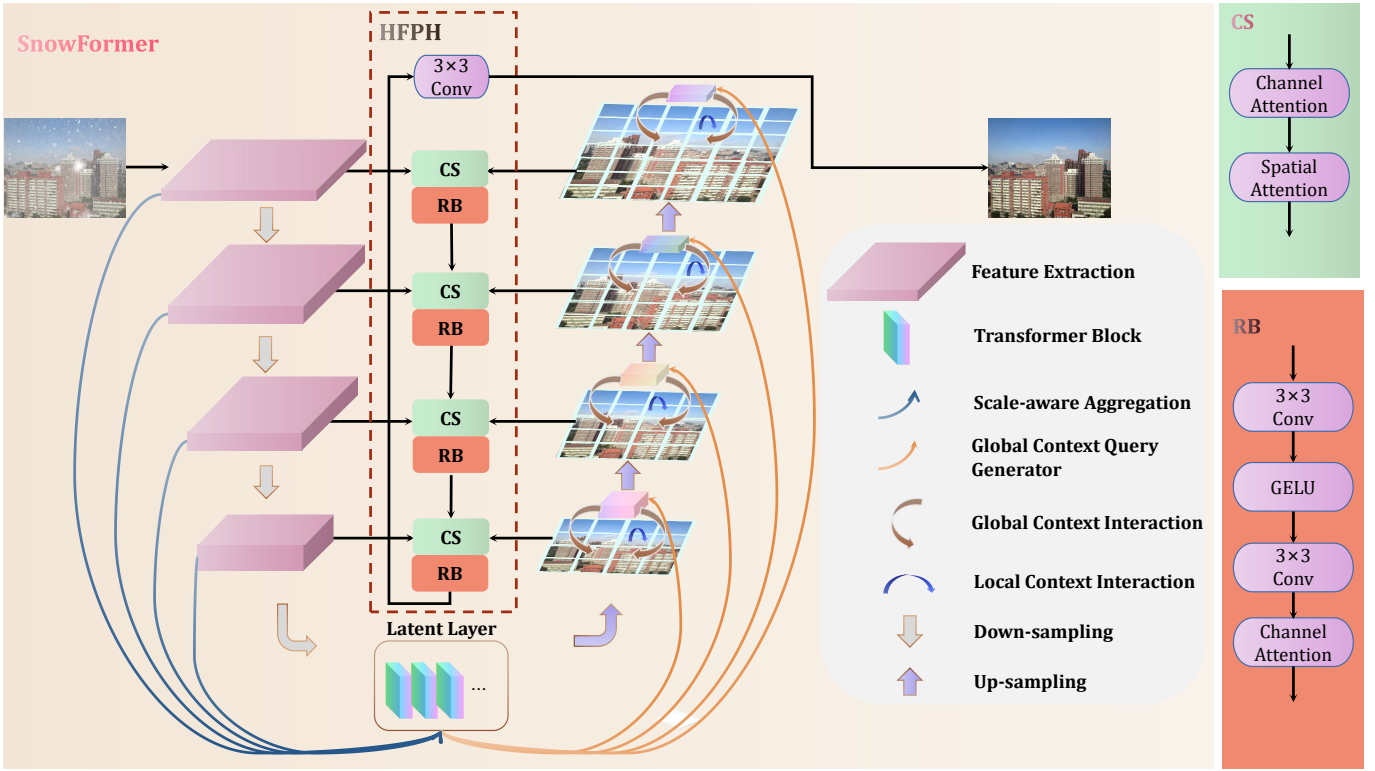


Figure 3: The overall framework of our SnowFormer, which is a u-shaped encoder-decoder architecture. Scale-aware Aggregation, Context Interaction, and Heterogeneous Feature Projection Head (HFPFH) are detailed in the “Method” section.

**Global Context Interaction Module** In addition to local context interaction, there still exist two aspects to be considered: (i) The large-scale degradations (snow veiling and plaque) need to apply the global view to recover the clean image. (ii) Lack of interaction between local details and global context. Therefore, we propose Global Context Interaction Module to solve these deficiencies.

The scale-aware feature after self-attention processing owns global snow degradation information representation. To assist in reconstructing the decoder segment, we exploit the global feature to develop the context interaction query, which performs cross-attention through its global context knowledge to support the reconstruction of the global information of the image. The proposed context interaction query is depicted in Fig.3. Specifically, given the scale-aware feature  $X_l \in \mathbb{R}^{\frac{H}{16} \times \frac{W}{16} \times 16C}$ , Conv1x1 and down-sampling are firstly applied to align its size with that of local windows. Next, We adopt the attention mechanism from the spatial (Qin et al. 2020) and channel (Hu, Shen, and Sun 2018) levels to adaptively project the context interaction query. Therefore, the context interaction query is formulated as:

$$\mathbf{Q}_{gi} \in \mathbb{R}^{H_w^i \times W_w^i \times 2^i C} = \text{CS}(X_l \in \mathbb{R}^{\frac{H}{16} \times \frac{W}{16} \times 16C} \downarrow), \quad (6)$$

wherein the  $\downarrow$  denotes the operation to align size, which consists of convolution and down-sampling. CS is the query generator, which includes channel and spatial attention operations.  $i$  denotes the  $i$ -th stage of the decoder.  $H_w^i$  and

$W_w^i$  are the height and width of local windows in  $i$ -th layer. This query is guided by the scale-aware feature in the latent layer, which can be made up for the global context interaction required in the snow removal task. To enhance the local and global interaction while lessening the computation, we utilize the global interaction query for cross self-attention. Compared with local context interaction, we leverage external global information representation to facilitate the context interaction of local details and global snow features. So far, our proposed global information interaction can be expressed as:

$$\text{Attn}_G(\mathbf{Q}_g, \mathbf{K}_l, \mathbf{V}_l) = \text{Softmax}\left(\frac{\mathbf{Q}_g \mathbf{K}_l^T}{\sqrt{d}} + p\right) \mathbf{V}_l, \quad (7)$$

where  $\mathbf{Q}_g$ ,  $\mathbf{K}_l$  and  $\mathbf{V}_l$  come from the scale-aware and local window-based feature.  $d$  and  $p$  denote the dimensionality of key and relative position embedding (Liu et al. 2021). For the feed-forward network, we follow the configuration of local context interaction.

### Heterogeneous Feature Projection Head

For complex large-scale degradation scene, the output features of decoder frequently include residual snow (Chen et al. 2020, 2021c). In order to alleviate such problem, previous approaches usually adopt a refinement block to process the output feature of the decoder at the highest resolution (Zamir et al. 2021). In our heterogeneous architec-

ture, we claim that the information from the encoder and decoder are both crucial for image desnowing. Thus a Heterogeneous Feature Projection Head is proposed which fully combines CNNs-based and ViT-based information flow to progressively refine features and project the refined features to the final clean image.

However, the heterogeneous features are misaligned at the spatial and the channel levels, which can seriously affect the refinement process in the case of high-resolution features. Therefore, we utilize the two-level attention mechanism for different feature maps. This operation can be expressed as follows:

$$X_{pi} = \text{CS}(X_{ei} + X_{di}), \quad (8)$$

where  $X_{ei}$  and  $X_{di}$  denote the  $i$ -th layer features of encoder and decoder. For the features of the different stages, we use up-sampling and  $\text{Conv}1 \times 1$  to align the size with that of the highest resolution feature map.  $X_{pi}$  represents the aligned feature which can be considered as residual snow degradations. Inspired by (He et al. 2016), we apply the channel attention and two  $3 \times 3$  convolutions to build our refinement block. It is worth mentioning that we progressively use the fusion strategy to refine the encoder-decoder features instead of summing them up all together. The progressive mechanism is more conducive to the fusion of the features from different layers. The Heterogeneous Feature Projection Head can be expressed as:

$$\begin{aligned} X_{ri+1} &= \text{RB}(X_{pi+1} + X_{ri}), \\ X_{r0} &= \text{RB}(X_{p0} + X_{d0}), \end{aligned} \quad (9)$$

$$I(X) = \text{Conv}3 \times 3(X_{r4}), \quad (10)$$

where the  $X_{ri}$  denotes the  $i$ -th refined feature, RB is the refinement block.  $\text{Conv}3 \times 3$  means the output operation, which projects the feature into the clean image.

### Overall Loss Function

For better training supervision, we adopt PSNR loss (Chen et al. 2021b) as our reconstruction loss. The loss function can be calculated as:

$$L_{psnr} = -\text{PSNR}(I(X), Y), \quad (11)$$

where  $I(X)$  and  $Y$  are the desnowing result and its corresponding ground-truth.

In addition, we consider that restoring the image from the perceptual level is also critical. We apply the perceptual loss to improve the effect of restoring. The perceptual loss can be expressed as follows:

$$L_{perceptual} = \sum_{j=1}^2 \frac{1}{C_j H_j W_j} \|\phi_j(I(X)) - \phi_j(Y)\|_1, \quad (12)$$

wherein the  $\phi_j$  represents the specified layer of VGG-19 (Simonyan and Zisserman 2014).  $C_j, H_j, W_j$  denote the channel numbers, height, and width of the feature map.

Our overall loss function can be expressed as:

$$L = \lambda_1 L_{psnr} + \lambda_2 L_{perceptual}, \quad (13)$$

where the  $\lambda_1$  and  $\lambda_2$  are set to 1 and 0.2 in our paper.

## Implementation

### Training Details

During the training phase, we train our model using the Adam optimizer with initial momentum set to 0.9 and 0.999. We initialize the learning rate to 0.0002 and use a cyclic learning rate adjustment with a maximum learning rate of 1.2 times the initial learning rate. We train with a data augmentation strategy, and randomly crop  $256 \times 256$  patches to train for 800 epochs for the snow removal task. For data augmentation, we employ horizontal flipping and randomly rotate the image to a fixed angle. We choose layers 1 and 3 of VGG19 (Simonyan and Zisserman 2014) for perceptual loss.

### SnowFormer Configuration

For a detailed description, we introduce our SnowFormer configuration. Specifically, the minimum feature size of our model is  $\frac{1}{16}$  of the original image size, and the number of dimensions at each stage is  $\{16, 32, 64, 128, 256\}$ . In the encoder part, we set the number of feature extraction blocks at each stage to  $\{4, 6, 7, 8\}$ , respectively, and the multiples of the ascending dimension in the spindle-shape is  $\{1, 2, 2, 2\}$ . In the latent layer, the number of transformer blocks is set to 8, and the head for multi-head self-attention is 16. In the decoder part, we set the number of Context interaction Transformer Blocks to  $\{4, 6, 7, 8\}$ , and the heads to  $\{1, 2, 4, 8\}$ . For the window size in each layer is set to  $8 \times 8$ . We utilize two CS operations to generate the global interaction query at each stage. In the Heterogeneous Feature Projection Head, we employ six refinement blocks for each refinement stage.

## Experiments

### Evaluation Metrics

We adopt the commonly used PSNR and SSIM (Wang et al. 2004) metrics to evaluate the snow removal performance in RGB color space for our all experiments, which follows the state-of-the-art single-image snow removal method (Chen et al. 2021c).

### Evaluation Datasets

To demonstrate the superior performance of our manner on desnowing task, we train and test our SnowFormer on CSD (Chen et al. 2021c), SRRS (Chen et al. 2020) and Snow100K (Liu et al. 2018) datasets, all training and testing dataset settings follow the latest published single image desnowing (Chen et al. 2020) to choose 2000 images on each testing dataset for a fair and convinced comparison.

### Quantitative Evaluation

In this subsection, we compare with the previous state-of-the-art approaches, including DesnowNet (Liu et al. 2018), CycleGAN (Engin, Genç, and Kemal Ekenel 2018), All in One (Li, Tan, and Cheong 2020), JSTASR (Chen et al. 2020), HDCW-Net (Chen et al. 2021c). In addition, to highlight our method’s excellent performance and compare in more detail, we retrain the general image restoration (NAFNet) and adverse weather restoration (TransWeather)

Table 1: Quantitative comparison of various desnowing approaches on the CSD (Chen et al. 2021c), SRRS (Chen et al. 2020) and Snow 100K (Liu et al. 2018) datasets. Underline and bold indicate the best metrics.

Method	CSD (2000)		SRRS (2000)		Snow 100K (2000)	
	PSNR $\uparrow$	SSIM $\uparrow$	PSNR $\uparrow$	SSIM $\uparrow$	PSNR $\uparrow$	SSIM $\uparrow$
(TIP'18)DesnowNet (Liu et al. 2018)	20.13	0.81	20.38	0.84	30.50	0.94
(CVPR'18)CycleGAN (Engin, Genç, and Kemal Ekenel 2018)	20.98	0.80	20.21	0.74	26.81	0.89
(CVPR'20)All in One (Li, Tan, and Cheong 2020)	26.31	0.87	24.98	0.88	26.07	0.88
(ECCV'20)JSTASR (Chen et al. 2020)	27.96	0.88	25.82	0.89	23.12	0.86
(ICCV'21)HDCW-Net (Chen et al. 2021c)	29.06	0.91	27.78	0.92	31.54	0.95
(CVPR'22)TransWeather (Valanarasu, Yasarla, and Patel 2022)	31.76	0.93	28.29	0.92	31.82	0.93
(ECCV'22)NAFNet (Chen et al. 2022)	<u>33.13</u>	<u>0.96</u>	<u>29.72</u>	<u>0.94</u>	<u>32.41</u>	<u>0.95</u>
SnowFormer (Ours)	<b>38.26</b>	<b>0.98</b>	<b>34.99</b>	<b>0.98</b>	<b>37.89</b>	<b>0.98</b>

methods to compare. The quantitative evaluation results are shown in Table 1. As shown in Table 1, our method outperforms all state-of-the-art approaches for snow removal, including general image restoration architectures and single image desnowing method (Chen et al. 2021c). On the CSD dataset, SnowFormer achieves the 4.95dB PSNR and 0.02 SSIM gain compared with the NAFNet and surpasses the HDCW-Net 9.02dB on the PSNR metric. Our method also attracts the 34.99dB PSNR and 0.98 SSIM on the SRRS dataset, which is higher than the second-best approach 5.27dB. Overall, our SnowFormer achieves a substantial lead in the three benchmarks for snow scenes compared with the SOTA methods.

### Qualitative Evaluation

The qualitative comparisons of state-of-the-art desnowing algorithms on real-world and synthetic snowy images are respectively revealed in Fig. 4 and Fig. 5. As observed in the red rectangle of Fig. 4, it is visually found that the recovered results by previous desnowing methods (Chen et al. 2020; Li, Tan, and Cheong 2020; Chen et al. 2021d; Valanarasu, Yasarla, and Patel 2022; Chen et al. 2022) still have residual snow spots and snow mark with small size. In comparison, our proposed method can remove multiple snow degradations with different size and provide more pleasant snow removal results with more details, which indicates the superior generalization ability on real-world scenes. Fig. 5 shows the visual comparisons on the synthetic snowy images selected from CSD dataset (Chen et al. 2021c). From Fig. 5, the results of JSTASR, All in one and HDCW-Net still have some large and non-transparent snow particles owing to its sufficient desnowing ability. Although TransWeather (Valanarasu, Yasarla, and Patel 2022) and NAFnet (Chen et al. 2022) can remove most snow particles with large size, the snow mark with small size cannot be removed effectively. Moreover, the occluded textural details are not recovered well. Compared with these SOTA methods, SnowFormer can achieve better desnowing performance for various degradation scales and the restored clear images are more closer to the ground truths.

### Ablation Study

To demonstrate the effectiveness of our proposed module, we perform the ablation experiments of SnowFormer. We train our model on image patches of size  $192 \times 192$  for 150

epochs on the CSD training dataset (Chen et al. 2021c), and test the effect on the CSD testing set. The other configurations are the same as described above. Next, we verify the effectiveness of each module separately.

### Improvements of Scale-aware Aggregation Module

In this part, we aim to demonstrate the gain from the Scale-aware Aggregation (SaA) operation. We remove the multi-scale feature aggregation and only use the feature processed down-sampling repeatedly for global modeling in the latent layer. The results are presented in Table 2. We found that the scale-aware aggregation improves the model's performance while increasing the computation and parameters to negligible. This is because the scale-aware feature enables the representation of various snow degradations without being lost due to the reduced feature map size.

Table 2: Ablation Study on Scale-aware Aggregation Module. Underline indicates the best metrics. (PSNR(dB)/SSIM)

Setting	Model	#Param	#GFLOPs	PSNR	SSIM
a	w/o SaA	8.32M	19.43G	30.86	0.956
b	w SaA (Ours)	8.35M	19.43G	<u>31.14</u>	<u>0.958</u>

### Effectiveness of Context Interaction Transformer Block

To demonstrate the effectiveness of components in our Context Interaction Transformer Block (CITB), we conduct the following ablation experiments: (i) We only use the local context interaction to replace the global context interaction. (LCI) (ii) We exploit the global context interaction and lack local information modeling. (GCI) (iii) Our proposed context interaction module, which utilizes the scale-aware feature to process global context cross-attention and combine the interaction with local information. (LGCI) Table 3 shows that interaction between local details and global context and local context interaction are vital for image desnowing, which achieves the visible gain compared to the single context interaction.

### Benefits of Heterogeneous Feature Projection Head

We analyze the benefits of the Heterogeneous Feature Projection Head in this section. Specifically, we verify the merits of our heterogeneous features compared to single feature input (Zamir et al. 2021). And the advantage of progressive

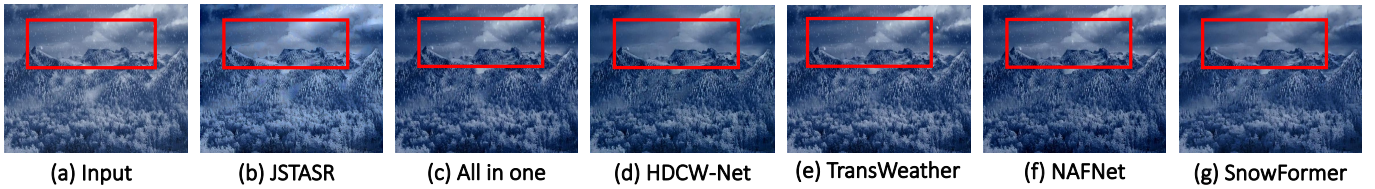


Figure 4: Visual comparison of state-of-the-art methods and SnowFormer on the real-world dataset (Ye et al. 2022). Please enlarge the image to observe details.

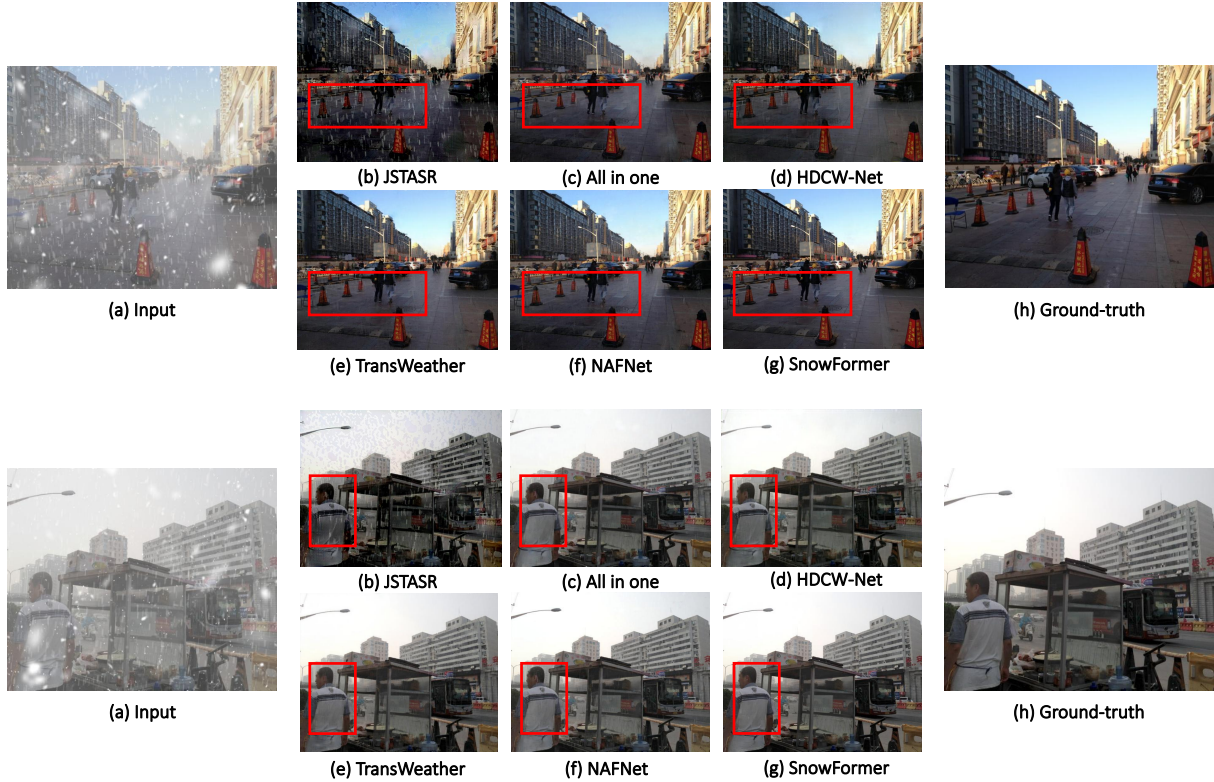


Figure 5: Visual comparison of state-of-the-art methods and SnowFormer on the CSD (Chen et al. 2021c) dataset. Please enlarge the image to see details.

Table 3: Ablation Study on Context Interaction Transformer Block. Underline indicates the best metrics. (PSNR(dB)/SSIM)

Setting	Model	#Param	#GFLOPs	PSNR	SSIM
a	LCI (Liu et al. 2021)	8.32M	19.62G	30.91	0.956
b	GCI	8.22M	19.22G	30.78	0.955
c	LGCI (Ours)	8.35M	19.43G	<u>31.14</u>	<u>0.958</u>

fusion over direct fusion. We conduct the following experiments to validate them: (i) We remove the Heterogeneous Feature Projection Head. (ii) We only use the last decoder feature for our refinement blocks. (FPH) (iii) We do fusion and refinement at once rather than progressively. (HFPH w/o progressively) (iv) We hierarchically fuse the feature of each encoder and decoder, and refine them progressively. (HFPH) The results are presented in Table 4. We observe that en-

coder and decoder heterogeneous features can improve the detailed refinement compared with the single feature. In addition, the progressively fuse operation is better than the direct fusion and refinement.

Table 4: Ablation Study on Heterogeneous Feature Projection Head. Underline indicates the best metrics. (PSNR(dB)/SSIM)

Setting	Model	#Param	#GFLOPs	PSNR	SSIM
a	w/o HFPH	8.22M	10.38G	30.34	0.947
b	FPH (Zamir et al. 2021)	8.25M	12.40G	30.62	0.951
c	HFPH w/o progressively	8.35M	18.98G	30.99	0.957
d	HFPH (Ours)	8.35M	19.43G	<u>31.14</u>	<u>0.958</u>

## Conclusion

In this paper, we propose a strong image snow removal network. It fully aggregates multi-scale degradation information and exploits Contextual Interactions to handle local and

large-scale snow scenes. At the highest resolution stage we utilize Heterogeneous Feature Projection Head to deal with the residual degradation problem. Huge gains are achieved in all three desnowing datasets, which demonstrate the superiority of our proposed model.

### Supplementary Material

This is a supplementary file for SnowFormer: Scale-aware Transformer via Context Interaction for Single Image Desnowing. In this supplementary material, we first introduce the detailed structure of our Transformer Block in the latent layer of our model. Next, we visualize the feature maps to demonstrate the effectiveness of the proposed Heterogeneous Feature Projection Head. Finally, we provide more visual comparisons to demonstrate the superiority of our SnowFormer.

We presents the following information that can be beneficial for the readers:

- Detailed Structure of Transformer Block in SnowFormer.
- Feature Visualization of Heterogeneous Feature Projection Head
- Additional visual comparison on real-world and synthetic snow images.

### Detailed Structure of Transformer Block in SnowFormer

Our Transformer Block consists of Self-attention (SA) and Multi-scale Feed-forward Network (MFFN). For the obtained scale-aware feature  $X_s \in \mathbb{R}^{H \times W \times C}$ , we reshape it to  $X_s \in \mathbb{R}^{N \times C}$  and adopt learnable  $W_Q^{C \times C}$ ,  $W_K^{C \times C}$  and  $W_V^{C \times C}$  to project the  $X_s$  into  $Q$  ( $XW_Q$ ),  $K$  ( $XW_K$ ) and  $V$  ( $XW_V$ ). In order to improve the local extraction ability, we add a  $3 \times 3$  depth-wise convolution. Therefore, Self-attention can be expressed as:

$$X'_s \in \mathbb{R}^{N \times C} = \text{Softmax} \left( \frac{QK^T}{\sqrt{C}} \right) \times V + \text{DWConv}(X_s), \quad (14)$$

where  $X'_s$  represents the scale-aware feature processed by SA.  $H$ ,  $W$  and  $C$  denote the height, width and dimension numbers of scale-aware feature.  $N$  is the number of token.  $\text{Softmax}(\cdot)$  is the the Softmax operation. In addition, we follow the (Dosovitskiy et al. 2020) to use multi-head self-attention for the above operations.

For the feed-forward network, we employ the proposed Multi-scale Feed-forward Network (MFFN) to improve the ability of local information extraction, which consists of multiple kernels convolution instead of a full connection layer for better performance, as shown in Fig.(6). Specifically, we use a  $1 \times 1$  convolution to expand features into high-dimension (Expand ratio is 2 in our paper). Next, we utilize  $3 \times 3$  and  $5 \times 5$  depth-wise convolutions to extract multi-scale information and apply Simple Gate (Chen et al. 2022) to replace GELU activation. We adopt  $1 \times 1$  convolution to reduce the dimension numbers before outputting the feature.

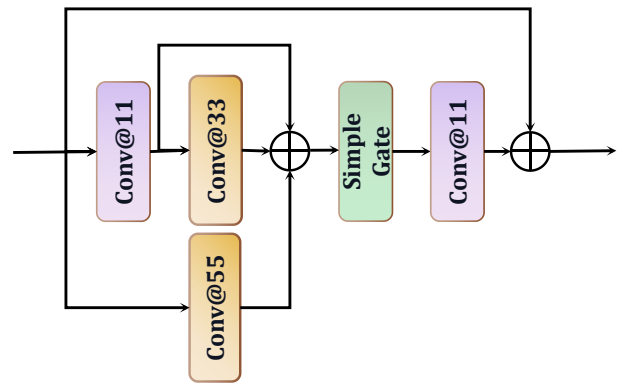


Figure 6: Detailed structure diagram of our Multi-scale Feed-forward Network (MFFN).

### Feature Visualization of Heterogeneous Feature Projection Head

To further demonstrate the effectiveness and necessity of our Heterogeneous Feature Projection Head, we visualize the feature maps in Fig. 7. We can observe that our proposed Heterogeneous Feature Projection Head can promote the refinement of residual degradation in the feature space.



Figure 7: The left map is the feature before being processed by the Heterogeneous Feature Projection Head. The right map is the feature after being processed by the Heterogeneous Feature Projection Head.

Fig.(8) is the feature maps from CNNs-based and ViT-based at the same stage. CNN feature focuses on sharp and strong edges, while Transformer pays attention to global low-frequency information recovery. Therefore, combining and refining the heterogeneous features on the Heterogeneous Feature Projection Head is crucial.

### Additional Visual Comparison

We present the additional visual comparison on synthetic and real snow images with other SOTA methods in Fig.(9). Worth noting that our method achieves more superior visual quality on both real and synthetic images, compared with other desnowing methods.

### References

Carion, N.; Massa, F.; Synnaeve, G.; Usunier, N.; Kirillov, A.; and Zagoruyko, S. 2020. End-to-end object detection with transformers. In *European conference on computer vision*, 213–229. Springer.



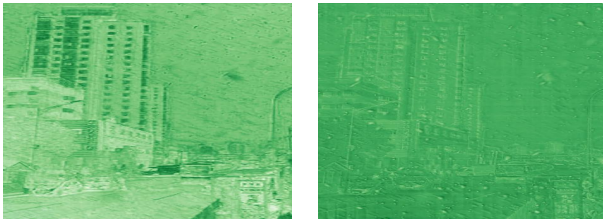


Figure 8: The picture on the left is the feature of the encoder part based on CNNs. The picture on the right is the feature of the ViT-based decoder.

Chen, C.-F. R.; Fan, Q.; and Panda, R. 2021. Crossvit: Cross-attention multi-scale vision transformer for image classification. In *Proceedings of the IEEE/CVF International Conference on Computer Vision*, 357–366.

Chen, J.; Lu, Y.; Yu, Q.; Luo, X.; Adeli, E.; Wang, Y.; Lu, L.; Yuille, A. L.; and Zhou, Y. 2021a. Transunet: Transformers make strong encoders for medical image segmentation. *arXiv preprint arXiv:2102.04306*.

Chen, L.; Chu, X.; Zhang, X.; and Sun, J. 2022. Simple baselines for image restoration. *arXiv preprint arXiv:2204.04676*.

Chen, L.; Lu, X.; Zhang, J.; Chu, X.; and Chen, C. 2021b. HINet: Half instance normalization network for image restoration. In *Proceedings of the IEEE/CVF Conference on Computer Vision and Pattern Recognition*, 182–192.

Chen, W.-T.; Fang, H.-Y.; Ding, J.-J.; Tsai, C.-C.; and Kuo, S.-Y. 2020. JSTASR: Joint size and transparency-aware snow removal algorithm based on modified partial convolution and veiling effect removal. In *European Conference on Computer Vision*, 754–770. Springer.

Chen, W.-T.; Fang, H.-Y.; Hsieh, C.-L.; Tsai, C.-C.; Chen, I.; Ding, J.-J.; Kuo, S.-Y.; et al. 2021c. ALL Snow Removed: Single Image Desnowing Algorithm Using Hierarchical Dual-Tree Complex Wavelet Representation and Contradict Channel Loss. In *Proceedings of the IEEE/CVF International Conference on Computer Vision*, 4196–4205.

Chen, W.-T.; Fang, H.-Y.; Hsieh, C.-L.; Tsai, C.-C.; Chen, I.; Ding, J.-J.; Kuo, S.-Y.; et al. 2021d. ALL Snow Removed: Single Image Desnowing Algorithm Using Hierarchical Dual-Tree Complex Wavelet Representation and Contradict Channel Loss. In *Proceedings of the IEEE/CVF International Conference on Computer Vision*, 4196–4205.

Dosovitskiy, A.; Beyer, L.; Kolesnikov, A.; Weissenborn, D.; Zhai, X.; Unterthiner, T.; Dehghani, M.; Minderer, M.; Heigold, G.; Gelly, S.; et al. 2020. An image is worth 16x16 words: Transformers for image recognition at scale. *arXiv preprint arXiv:2010.11929*.

Engin, D.; Genç, A.; and Kemal Ekenel, H. 2018. Cycledehaze: Enhanced cyclegan for single image dehazing. In *Proceedings of the IEEE conference on computer vision and pattern recognition workshops*, 825–833.

He, K.; Zhang, X.; Ren, S.; and Sun, J. 2016. Deep residual learning for image recognition. In *Proceedings of the*

*IEEE conference on computer vision and pattern recognition*, 770–778.

Hu, J.; Shen, L.; and Sun, G. 2018. Squeeze-and-excitation networks. In *Proceedings of the IEEE conference on computer vision and pattern recognition*, 7132–7141.

Lee, H.; Choi, H.; Sohn, K.; and Min, D. 2022. KNN Local Attention for Image Restoration. In *Proceedings of the IEEE/CVF Conference on Computer Vision and Pattern Recognition*, 2139–2149.

Lee, Y.; Kim, J.; Willette, J.; and Hwang, S. J. 2021. MPViT: Multi-Path Vision Transformer for Dense Prediction. *arXiv preprint arXiv:2112.11010*.

Li, R.; Tan, R. T.; and Cheong, L.-F. 2020. All in one bad weather removal using architectural search. In *Proceedings of the IEEE/CVF Conference on Computer Vision and Pattern Recognition*, 3175–3185.

Liu, Y.-F.; Jaw, D.-W.; Huang, S.-C.; and Hwang, J.-N. 2018. DesnowNet: Context-aware deep network for snow removal. *IEEE Transactions on Image Processing*, 27(6): 3064–3073.

Liu, Z.; Lin, Y.; Cao, Y.; Hu, H.; Wei, Y.; Zhang, Z.; Lin, S.; and Guo, B. 2021. Swin transformer: Hierarchical vision transformer using shifted windows. In *Proceedings of the IEEE/CVF International Conference on Computer Vision*, 10012–10022.

Mehta, S.; and Rastegari, M. 2021. Mobilevit: light-weight, general-purpose, and mobile-friendly vision transformer. *arXiv preprint arXiv:2110.02178*.

Pei, S.-C.; Tsai, Y.-T.; and Lee, C.-Y. 2014. Removing rain and snow in a single image using saturation and visibility features. In *2014 IEEE International Conference on Multi-media and Expo Workshops (ICMEW)*, 1–6. IEEE.

Qin, X.; Wang, Z.; Bai, Y.; Xie, X.; and Jia, H. 2020. FFA-Net: Feature fusion attention network for single image dehazing. In *Proceedings of the AAAI Conference on Artificial Intelligence*, volume 34, 11908–11915.

Ronneberger, O.; Fischer, P.; and Brox, T. 2015. U-net: Convolutional networks for biomedical image segmentation. In *International Conference on Medical image computing and computer-assisted intervention*, 234–241. Springer.

Simonyan, K.; and Zisserman, A. 2014. Very deep convolutional networks for large-scale image recognition. *arXiv preprint arXiv:1409.1556*.

Song, Y.; He, Z.; Qian, H.; and Du, X. 2022. Vision Transformers for Single Image Dehazing. *arXiv preprint arXiv:2204.03883*.

Valanarasu, J. M. J.; Yasarla, R.; and Patel, V. M. 2022. Transweather: Transformer-based restoration of images degraded by adverse weather conditions. In *Proceedings of the IEEE/CVF Conference on Computer Vision and Pattern Recognition*, 2353–2363.

Wang, W.; Xie, E.; Li, X.; Fan, D.-P.; Song, K.; Liang, D.; Lu, T.; Luo, P.; and Shao, L. 2021. Pyramid vision transformer: A versatile backbone for dense prediction without convolutions. In *Proceedings of the IEEE/CVF International Conference on Computer Vision*, 568–578.

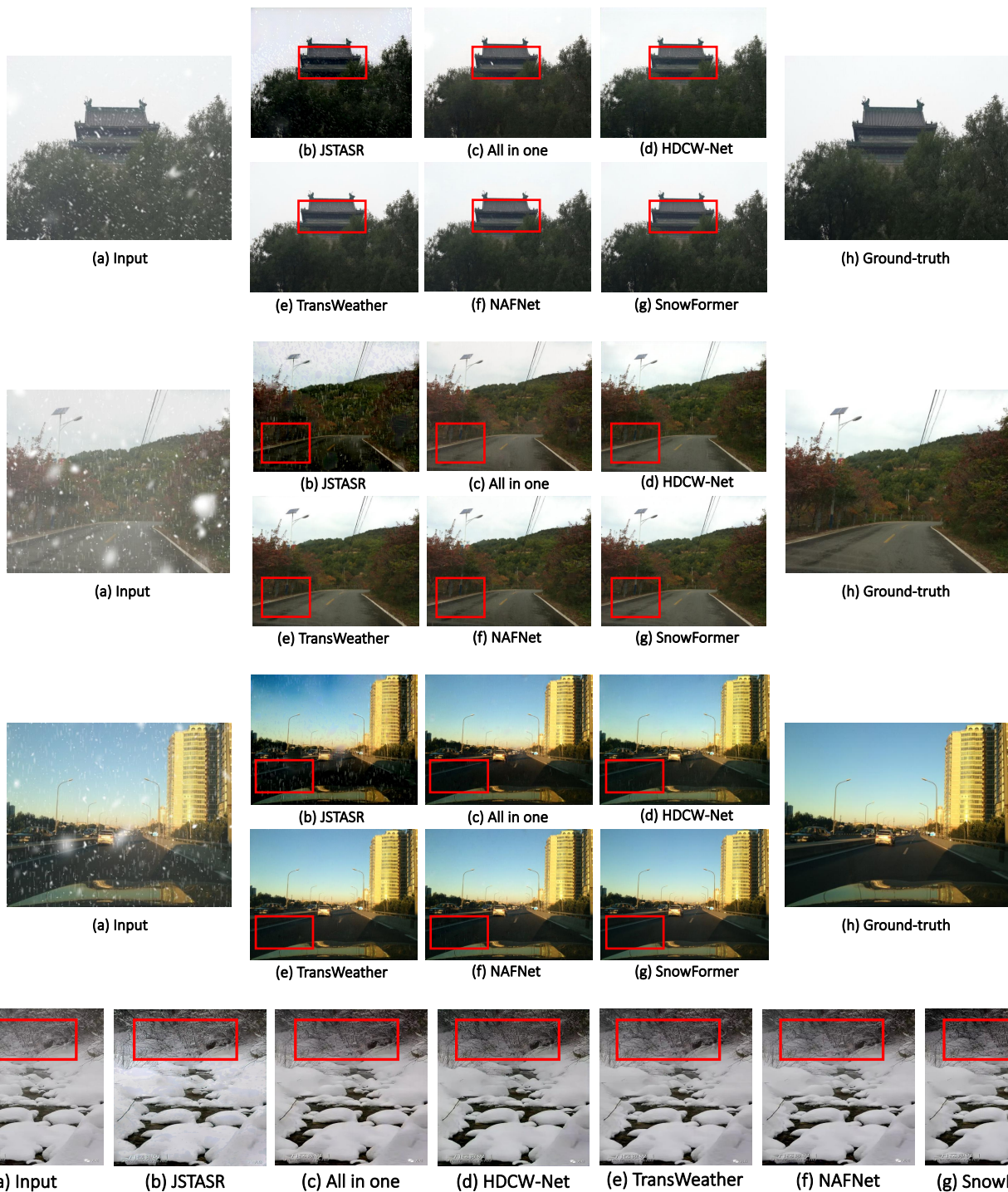


Figure 9: Visual comparison of state-of-the-art methods and SnowFormer on the CSD (Chen et al. 2021c) and real-world datasets (Ye et al. 2022). Please enlarge the image to see details.

Wang, Y.; Liu, S.; Chen, C.; and Zeng, B. 2017. A hierarchical approach for rain or snow removing in a single color image. *IEEE Transactions on Image Processing*, 26(8): 3936–3950.

Wang, Z.; Bovik, A. C.; Sheikh, H. R.; and Simoncelli, E. P.

2004. Image quality assessment: from error visibility to structural similarity. *IEEE transactions on image processing*, 13(4): 600–612.

Wang, Z.; Cun, X.; Bao, J.; Zhou, W.; Liu, J.; and Li, H. 2022. Uformer: A general u-shaped transformer for image

restoration. In *Proceedings of the IEEE/CVF Conference on Computer Vision and Pattern Recognition*, 17683–17693.

Ye, T.; Chen, S.; Liu, Y.; Chen, E.; and Li, Y. 2022. Towards Efficient Single Image Dehazing and Desnowing. *arXiv preprint arXiv:2204.08899*.

Zamir, S. W.; Arora, A.; Khan, S.; Hayat, M.; Khan, F. S.; and Yang, M.-H. 2021. Restormer: Efficient Transformer for High-Resolution Image Restoration. *arXiv preprint arXiv:2111.09881*.

Zheng, X.; Liao, Y.; Guo, W.; Fu, X.; and Ding, X. 2013. Single-image-based rain and snow removal using multi-guided filter. In *International conference on neural information processing*, 258–265. Springer.